Barbara Surowska*, Monika Ostapiuk

Lublin University of Technology, Faculty of Mechanical Engineering, ul. Nadbystrzycka 36, 20-618 Lublin, Poland
Corresponding author. E-mail: b.surowska@pollub.pl

CHARACTERIZATION OF GFRP INTERLAYER AS BARRIER LAYER IN Al/CFRP LAMINATE

Carbon fibre reinforced polymers (CFRPs) are an attractive construction material with an increasingly wide scope of application, including the aircraft industry. By combining them with metal elements and producing fibre metal laminates (FMLs), it is possible to achieve higher mechanical properties than in the case of combinations with glass fibre reinforced polymer (GFRP). However, there is a problem associated with galvanic corrosion regarding combinations with aluminium and its alloys, stainless steel and with magnesium alloys because CFRP composites are electrical conductors. Adhesives with increasingly higher resistivity are applied in adhesive bonding technology. Fibre metal laminates (FMLs), particularly those dedicated for aircraft primary structures must be not only corrosion resistant, but first of all they must be characterized by a proper combination of mechanical properties, including fatigue features. Therefore, when designing the metal surface treatment and the type of interlayers, it is necessary to consider the joint adhesion, mechanical properties of the hybrid laminate and corrosion properties. This article presents the characterization of an interface microstructure: the anodic layer on the AA 2024 aluminium alloy-GFRP-CFRP interlayer of hybrid laminates with electrical properties presented in a previous publication. The observations have been carried out on cross-sections of Al/GFRP-R/CFRP, Al/GFRP-S/CFRP and Al/CFRP laminates in a 2/1 layout with fibres oriented in the 0° direction. Moreover, impedance measurement was performed for the oxide layer in contact with a 3.5% aqueous NaCl solution by means of electrochemical impedance spectroscopy (EIS). It has been found that the low contact resistivity between the laminate with the GFRP-S interlayer was caused by carbon fibre migration to the Al/GFRP-S boundary. Furthermore, the low surface resistance of the CFRP composite and the porosity of the outer part of the oxide layer on aluminium enables the diffusion of aggressive ions and migration of electrical charge towards the metal substrate, which poses a threat of corrosion initiation in moisture condensation conditions.

Keywords: CFRP, FML hybrid laminates, a GFRP interlayer, EIS, interface microstructure

CHARAKTERYSTYKA MIĘDZYWARSTWY GFRP JAKO WARSTWY IZOLACYJNEJ W LAMINACIE Al/CFRP

Kompozyty polimerowe wzmacniane włóknem węglowym (CFRP) są atrakcyjnym materiałem konstrukcyjnym o coraz szerszym zastosowaniu, w tym w lotnictwie. Łączenie ich z elementami metalowymi oraz wytwarzanie laminatów metalowo--włóknistych (FML) pozwala na uzyskanie wyższych właściwości mechanicznych od połączeń z kompozytem wzmacnianym włóknem szklanym (GFRP). Niestety, dla połączeń z aluminium i jego stopami, stalą nierdzewną, stopami magnezu problemem jest korozja galwaniczna, ponieważ kompozyty CFRP są przewodnikami prądu. Do łączenia technologią klejenia stosuje się kleje o coraz wyższej rezystywności. FML przeznaczone zwłaszcza na lotnicze struktury pierwszorzędowe (ang. aircraft primery structures) muszą nie tylko być odporne na korozję, ale przede wszystkim muszą mieć odpowiedni zestaw właściwości mechanicznych, w tym zmęczeniowych. Dlatego projektowanie obróbki powierzchni metalu i rodzaju międzywarstw musi uwzględniać adhezję połączenia, właściwości mechaniczne hybrydowego laminatu i właściwości korozyjne. W artykule przedstawiono badania mikrostruktury interfejsu: warstwa anodowa na stopie aluminium AA 2024-międzywarstwa GFRP-CFRP laminatów hybrydowych o właściwościach elektrycznych przedstawionych we wcześniejszej publikacji. Obserwacje wykonano na przekrojach laminatów Al/GFRP-R/CFRP, Al/GFRP-S/CFRP oraz Al/CFRP w układzie 2/1 z włóknem w kierunku 0°. Ponadto wykonano pomiar impedancji dla warstwy tlenkowej w kontakcie z 3.5% wodnym roztworem NaCl metodą elektrochemicznej spektroskopii impedancyjnej (EIS). Stwierdzono, że przyczyną niskiej rezystywności kontaktowej laminatu z międzywarstwą GFRP-S była migracja włókna węglowego do granicy Al/GFRP-S. Ponadto niska rezystancja powierzchniowa kompozytu CFRP i porowatość zewnętrznej części warstwy tlenkowej na aluminium umożliwia dyfuzję agresywnych jonów i wędrówkę ładunku elektrycznego w kierunku podłoża metalowego, co stwarza zagrożenie inicjowania korozji w warunkach kondensacji wilgoci.

Słowa kluczowe: CFRP, hybrydowe laminaty FML, międzywarstwa GFRP, EIS, mikrostruktura interfejsu

INTRODUCTION

Carbon fibre reinforced polymers (CFRPs) are an attractive construction material with an increasingly wide scope of application, including the aircraft industry. By combining them with metal elements and

producing fibre metal laminates (FMLs), it is possible to achieve higher mechanical properties than in the case of combinations with glass fibre reinforced polymer (GFRP) [1, 2]. Unfortunately, there is a problem associated with galvanic corrosion regarding combinations with aluminium and its alloys, stainless steel and with magnesium alloys because CFRP composites are electrical conductors. Adhesives with increasingly higher resistivity are applied in adhesive bonding technology. Fibre metal laminates (FMLs), particularly those dedicated for aircraft primary structures must be not only corrosion resistant, but first of all they must be characterized by a proper combination of mechanical properties, including fatigue features [2-4]. Therefore, when designing the metal surface treatment and the type of interlayers, it is necessary to consider the joint adhesion and mechanical properties of the hybrid laminate as well as the corrosion properties [2, 5].

The anodizing process combined with surface sealing is the most effective method of corrosion reduction in aluminium alloys [6, 7]. Such a metal surface for bonding with composites in the autoclave process is not an optimal method in terms of joint adhesion. Therefore, in GLARE (Al/GFRP), primer layers are usually used to seal the anodic coating or the anodizing process is substituted by sol-gel coatings. However, no effective methods of galvanic corrosion prevention have been developed yet for Al/CFRP laminates, despite research being carried out [8-10] and therefore their present application is limited.

The results of research in the scope of the electrical properties of the components and FMLs characterized by application of the aluminium anodizing process and by GFRP laminates as an isolating barrier were presented in a previous study [11] published by the authors. However, the low resistivity obtained on the boundary in a laminate with a thin layer of glass prepreg and the preliminary results of tests in a salt spray chamber were not satisfactory, therefore an attempt to explain the reasons for the insufficient protective properties has been presented in this article.

MATERIALS AND EXPERIMENTAL MEASUREMENTS

The tests were carried out on the metal sheet and on the hybrid metal-fibre laminates with a 2/1 lay-out. The prepreg layers were arranged in the 0° direction. The aluminium alloy sheet was anodized in a sulphuric acid solution (SAA process).

The configuration of the samples is presented in Table 1.

The hybrid laminates were cured in the autoclave process using the parameters recommended by the prepreg manufacturers. The electrical properties of the components tested earlier on the basis of the ASTM D257 standard [12] revealed that the aluminium oxide and GFRP-R composite are insulators with a very high

surface resistivity of about $1 \cdot 10^{11}$ $\Omega/^2$ and $1.83 \cdot 10^{12}$ $\Omega/^2$ respectively, and the GFRP-S composite is also an insulator but its surface resistivity is lower ($2.56 \cdot 10^7$ $\Omega/^2$) [11]. It results from the difference in the epoxy resin.

TABLE 1. **Configuration of samples**
TABELA 1. **Konfiguracja próbek**

Sample	Components	Thickness and number of layers			
		Metal sheet	CFRP	GFRP-R	GFRP-S
Al	AA 2024 T3 (AlCu4Mg1) + SAA	0.5 mm/1	-	-	-
Al/CFRP	AA 2024 (SAA) HexPlyAS7/M12 UD carbon prepreg (Hexcel, USA)	0.5 mm/2	0.131 mm/4	-	-
Al/GFRP-R/CFRP	AA 2024 (SAA) HexPly M12TVR380/26% UD R-glass prepreg (Hexcel, USA) HexPlyAS7/M12 UD carbon prepreg (Hexcel, USA)	0.5 mm/2	0.131 mm/4	0.255 mm/1	-
Al/GFRP-S/CFRP	AA 2024 (SAA) RC45 S-glass UD prepreg (Axiom) HexPlyAS7/M12 UD carbon prepreg (Hexcel, USA)	0.5 mm/2	0.131 mm/4	-	0.13 mm/1

Impedance measurements for the aluminium oxide after AA 2024 anodizing in SAA were carried out by means of an Atlas 0531 potentiostat (Atlas-Sollich, Poland) with an FRA (Frequency Response Analyzer) and subjected to direct analysis in the measurement program. The employed amplitude of the sinusoidal signal was 10 mV and the frequency span was 100 kHz - 1 Hz. The tests were carried out in 3.5% NaCl (pH 6.5) and at ambient temperature (RT). The three-electrode cell consisted of the sample, a saturated calomel electrode (SCE) and platinum electrode as the working, reference and counter electrodes, respectively.

Microstructure observation was carried out using a light microscope (NIKON MA200, Olympus) and a scanning electron microscope (NovaNanoSEM 450, FEI). The samples were prepared in accordance with Struers and Buehler methodology. A gold layer 10 nm thick was applied for scanning observation.

RESULTS AND DISCUSSION

In the first phase of our research [11] a significant difference in the metal-GFRP contact resistivity value between the FML samples with glass fibre R and S composite, $1.84 \cdot 10^{12}$ and $1.62 \cdot 10^2$ $\Omega \cdot cm^2$, respectively, and current oscillation for the anodic layer were observed. Therefore, additional tests were carried out

using the method of electrochemical impedance spectroscopy (EIS) for the oxide layer and micro-structure observations on cross-sections of the laminates.

The impedance spectrum has been presented in the form of Nyquist and Bode plots (Fig. 1b). Diagram interpretation was based on an equivalent circuit (Fig. 1c). It is a typical diagram for metal with a protective layer subjected to a degradation (corrosion) process [13].
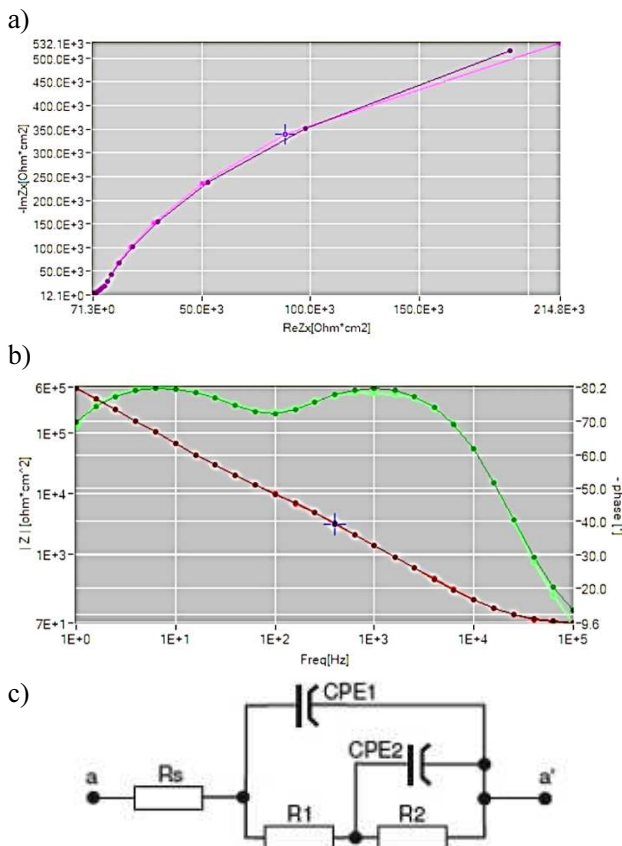
a)

b)

c)

Fig. 1. Impedance spectrum of anodic layer on AA 2024 T3: a) Nyquist plot, b) Bode plots, c) equivalent circuit

Rys. 1. Widmo impedancyjne warstwy anodowej na AA 2024: a) wykres Nyquista, b) wykres Bodego, c) obwód zastępczy

The impedance spectra show two similar time constants: the first one at high frequency (10 kHz) with a maximum phase angle of 80° in the Bode plot, and a second one at low frequency (about 8 Hz) with a similar phase angle (Fig. 1b). According to Ahuir--Torres [14], this second time constant is viewed as

a diffusion tail in the Nyquist diagram (Fig. 1a). The obtained shape of Nyquist plot indicates the prevailing mass transport process at negligible resistance of charge transfer in comparison with electrolyte resistance in the tested frequency range. From the impedance module of the Bode plot it is possible to obtain the electrolyte resistance in the high frequencies range Rs, whose value is equal to ~70 $\Omega \cdot cm^2$. The high value of impedance module for low frequencies and wide plateau from the phase angle maximum exceeding 800 indicate the high corrosion resistance of the oxide layer. The occurrence of the second time constant may be associated with pitting corrosion of the layer or with ion penetration into the layer pores [15-17]. To model the behaviour of the anodized surface of the aluminium alloy, the equivalent circuit shown in Figure 1c is proposed. This circuit comprised electrolyte resistance Rs, in series with a constant phase element CPE1, representing the oxide layer capacitance, which is parallel with resistance R1, representing the resistance of this layer. This resistance R1 is in series with a constant phase element CPE2, representing the capacitance of the porous part layer (diffusive process observed at low frequency). The n1 exponent of CPE1 and n2 exponent of CPE2 present the values of 0.95 and 0.92, respectively, which indicate that these constant phase elements are associated with the capacitors. Resistance R2 represents the porous layer resistance or the charge transfer resistance [15]. The porosity of the oxide layer produced in the anodizing process is its distinctive feature. The layers are not sealed in the FML production process. Figures 2-7 illustrate the microstructures of laminates being tested. Panoramic views have been presented in the form of sequences of photos from larger areas of the samples (Figs. 2, 4, 6) and microstructures from specific locations (Figs. 3, 5, 7). The panoramic pictures illustrate the fibres arranged in the 0° direction and the number of prepreg layers is visible (Figs. 2, 4, 6). Additionally, the oxide layer (SAA) is visible on the SEM images. The Al/CFRP laminate is characterized by a thin resin layer with an irregular thickness on the metal-composite boundary (Fig. 3). The carbon fibres move towards the oxide layer. Such an interface structure, if the anodic layer is unsealed, is an insufficient barrier to the flow of electric charges, which is responsible for the corrosion process in a humid environment.
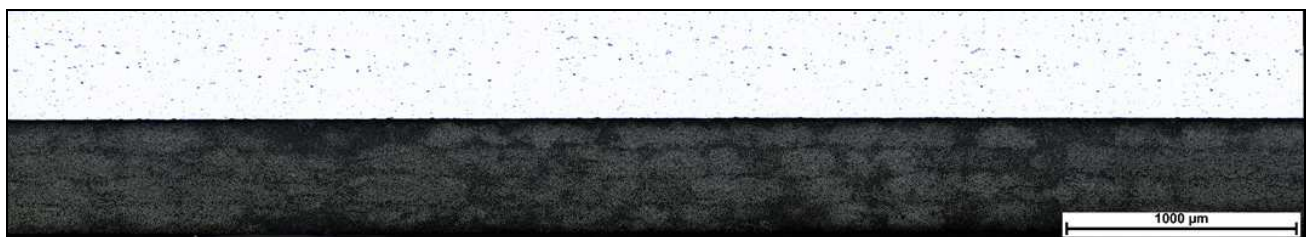

Fig. 2. Panoramic view of Al/CFRP laminate microstructure; light microscope

Rys. 2. Mikrostruktura Al/CFRP, obraz panoramiczny; mikroskop optyczny
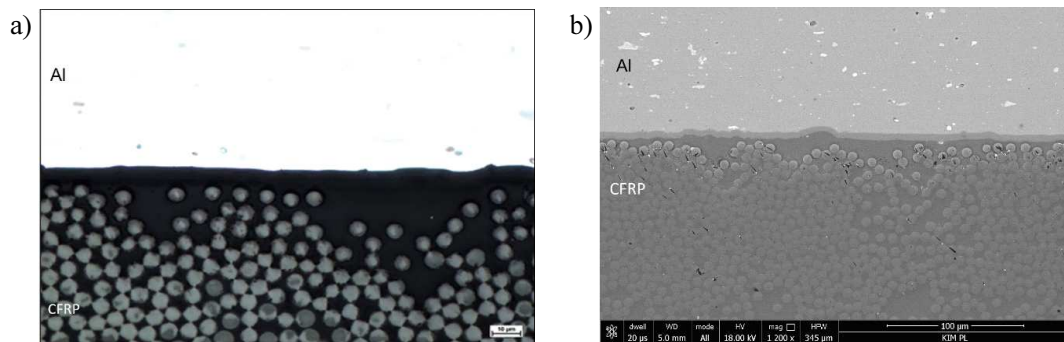
Fig. 3.   Microstructure of Al/CFRP laminate in: a) light microscope and b) SEM

Rys. 3.   Mikrostruktura laminatu Al/CFRP w: a) mikroskopie optycznym, b) SEM

In the Al/GFRP-R/CFRP laminate, the glass-carbon composite boundary is continuous but it is characterized by waviness (Fig. 4). The uniformity of the polymer matrix and full interface continuity is visible at higher magnifications (Fig. 5). The thickness of the glass prepreg is sufficient to insulate the carbon prepreg from the metal surface. In the Al/GFRP-S/CFRP laminate, the layer of applied glass prepreg with S fibre is thinner and a continuous joint has been achieved between the prepregs and between the composite and metal (Figs. 6 and 7). Unfortunately, waviness occurred in the course of the autoclave curing process in the carbon prepreg layer as well as in the Al/GFRP-R/CFRP laminate. Therefore, local movement of the carbon fibres towards the boundary with the metal occurred at a smaller thickness of GFRP-S glass composite (Fig. 7).
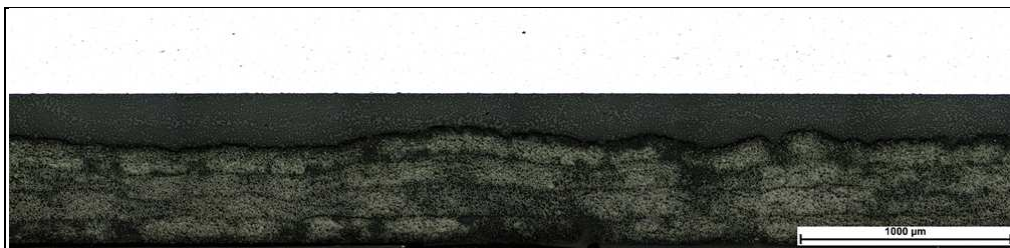

Fig. 4.   Panoramic view of Al/GFRP-R/CFRP laminate microstructure; light microscope

Rys. 4.   Mikrostruktura laminatu Al/GFRP-R/CFRP, obraz panoramiczny; mikroskop optyczny
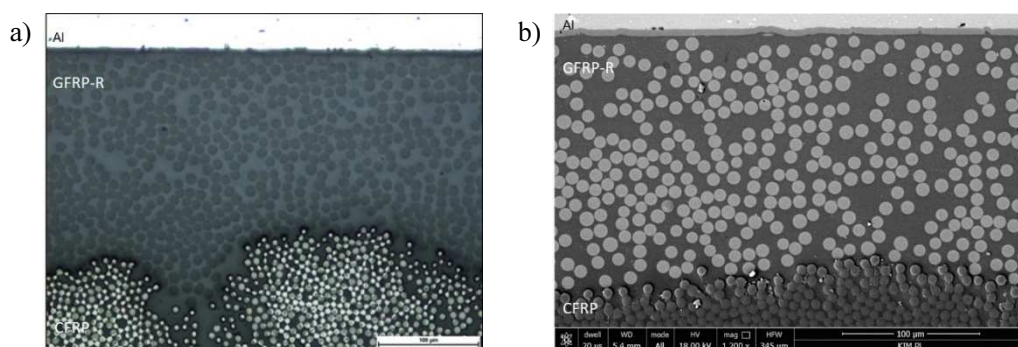

Fig. 5.   Al/GFRP-R/CFRP laminate microstructure in: a) light microscope and b) SEM

Rys. 5.   Mikrostruktura laminatu Al/GFRP-R/CFRP w: a) mikroskopie optycznym, b) SEM
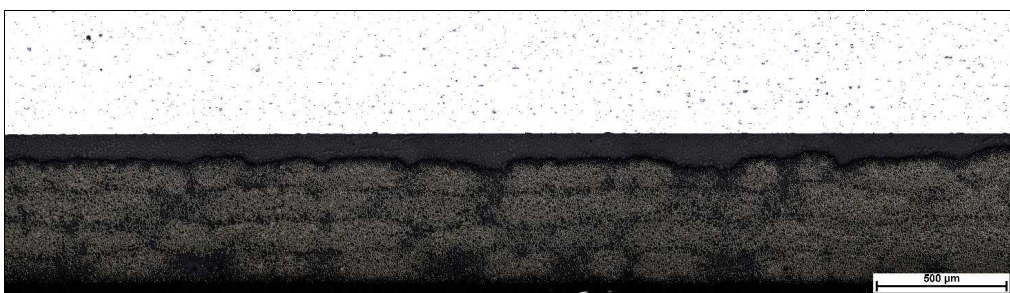

Fig. 6.   Panoramic view of Al/GFRP-S/CFRP laminate microstructure; light microscope

Rys. 6.   Mikrostruktura laminatu Al/GFRP-S/CFRP, obraz panoramiczny; mikroskop optyczny
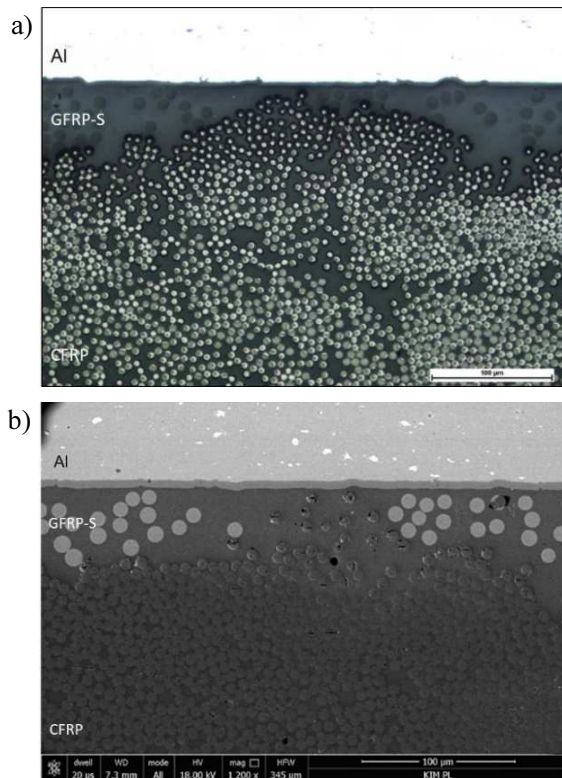
a)

b)

Fig. 7. Al/GFRP-S/CFRP laminate microstructure in: a) light microscope and b) SEM

Rys. 7. Mikrostruktura laminatu Al/GFRP-S/CFRP w: a) mikroskopie optycznym, b) SEM

Warpage of the flat laminates and distortion of the prepreg plies are specific to autoclave technology but the reasons for these deformations are not clearly described [18-20]. Various material and technological factors are taken into consideration. However, the influence of the difference in the physicochemical properties of the polymer matrix suggested by some authors has been not confirmed in research carried out by Stefaniak et al. [18] and cannot be recognized as significant because ply distortion has been observed in the CFRP/GFRP-R system in which both prepregs have the same matrix - M12 resin. A certain role can be played by the difference in diameter of the carbon and glass fibres in the UD 0° configuration but it cannot be treated as the basic factor because deformation is also observed in other laminates than hybrids. The most probable factor is the impact of the tool-laminate interaction due to a mismatch between the tool and the laminate coefficient of thermal expansion (CTE). As a consequence of this mismatch and due to the autoclave pressure forcing the laminate and tooling together, non-uniform stress distribution is observed [19, 20]. The cited studies were carried out on CFRP and GFRP laminates. For FML hybrid laminates, it can be assumed that the outer metal layers are the equivalent of tools. Therefore, the differences in the thermal properties of aluminium alloys as well as glass and carbon composites can be the main reason for the non-uniform distribution of stress and deformation in the autoclave curing process.

CONCLUSIONS

The phenomenon of low contact resistivity in Al/GFRP-S observed in electrical measurements can be explained by local displacements of the prepreg with carbon fibre revealed in local microstructures and depleting the dielectric GFRP layer in the boundary area. Discontinuity of the glass prepreg layer observed in microscopic examinations and the possibility of ion transport through the oxide layer demonstrated in EIS measurements can be the reason for the occurrence of corrosion on the metal-composite interface in operating conditions characterized by the presence of moisture condensation.

Acknowledgements

REFERENCES

[1] Surowska B., Jakubczak P., Bieniaś J., Structure and chemistry of fibre metal laminates, [in:] Hybrid Polymer Composite Materials: Structure and Chemistry, eds. V.K. Thakur, M.K. Thakur, R.K. Gupta, Chapter 8, Woodhead Publishing 2017, 193-234.
[2] Alderliesten R., Fatigue and Fracture of Fibre Metal Laminates, Springer International Publishing AG 2017.
[3] Botelho E.C., Silva R.A., Pardini L.C., Rezende M.C., A review on the development and properties of continuous fibre/epoxy/aluminium hybrid composites for aircraft structures, Mater. Res. 2006, 9, 247-256.
[4] Bieniaś J., Jakubczak P., Surowska B., Properties and characterization of fibre metal laminates, [in:] Hybrid Polymer Composite Materials: Properties and Characterisation, ed. V.K. Thakur, M.K. Thakur, A. Pappu, Chapter 11, Woodhead Publishing, 2017, 253-277.
[5] Sinmazcelik T., Avcu E., Bora M.O., Coban O., A review: Fibre metal laminates background, bonding types and applied test methods, Mater. Des. 2011, 32, 3671-3685.
[6] Vargel C., Jacques M., Schmidt M.P., Corrosion of Aluminium, Elsevier 2004.
[7] Dursun T., Soutis C., Review: Recent developments in advanced aircraft aluminium alloys, Materials and Design 2014, 56, 862-871
[8] Damato C.A., Botelho E.C., Rezende M.C., Influence of the environmental conditioning on the fatigue behaviour of carbon fibre/epoxy/aluminium laminates, [In:] 13th European Conference on Composite Materials, Stockholm, Sweden, 2008.
[9] Cai B.P., Liu Y.H., Ren C.K., Liu Z.K., Tian X.J., Abulimiti A.B., Experimental study of galvanic corrosion behaviour of carbon fibre composite coupled to aluminium in artificial seawater, Corrosion Engineering, Science and Technology 2012, 47(4), 289-296.
[10] Liu Z., Curioni M., Jamshidi P., Walker A., Prengnell P., Thompson G.E., Skeldon P., Electrochemical characteristics of a carbon fibre composite and the associated galvanic effects with aluminium alloys, Applied Surface Science 2014, 314, 233-240.
[11] Surowska B., Ostapiuk M., Electrical properties of aluminium-fibre reinforced composite laminates, Composites Theory and Practice 2016, 16, 4, 223-229.

[12] ASTM D257-99 Test Methods for DC Resistance or Conductance of Insulating Materials.

[13] Trzaska M., Trzaska Z., Elektrochemiczna spektroskopia impedancyjna w inżynierii materiałowej, Oficyna Wydawnicza Politechniki Warszawskiej, Warszawa 2010.

[14] Ahuir-Torres J.I., Arenas M.A., Perrie W., Dearden G., de Damborene J., Surface texturing of aluminium alloy AA2024-T3 by picosecond laser: Effect on wettability and corrosion properties, Surface & Coatings Technology 2017, 321, 279-291.

[15] Cheng Y.L., Zhang Z., Cao F.H., Li J.F., Zhang J.Q., Wang J.M., Cao C.N., A study of the corrosion of aluminium alloy 2024-T3 under thin electrolyte layers, Corrosion Science 2004, 46, 1649-1667.

[16] Gobara M., Kamel H., Akid R., Baraka A., Corrosion behaviour of AA2024 coated with an acid-soluble collagen/hybrid silica sol-gel matrix, Progress in Organic Coatings 2015, 89, 57-66.

[17] Palomino L.E.M., Suegama P.H., Aoki I.V., Paszti Z., de Melo H.G., Investigation of the corrosion behaviour of a bilayer cerium-silane pre-treatment on Al 2024-T3 in 0.1M NaCl, Electrochemica Acta 2007, 52, 7496-7505.

[18] Stefaniak D., Kappel E., Spröwitz T., Hühne C., Experimental identification of process parameters inducing warpage of autoclave-processed CFRP parts, Composites: Part A 2012, 43, 1081-1091.

[19] Twigg G., Poursartip A., Fernlund G., Tool-part interaction in composites processing. Part I: experimental investigation and analytical model. Composites Part A 2004, 35, 121-133.

[20] Radford D., Cure shrinkage induced warpage in flat uniaxial composites, Journal of Composite Technology and Research 1993, 15, 290-296.